Supplementary Information Chemical Communication

High Charge Carrier Mobility and Efficient Charge Separation in Highly Soluble Perylenetetracarboxyl-diimides

D. Deniz Günbaş,[†] Chenming Xue, [§] Sameer Patwardhan,[†] Maria C. Fravventura,[†] Hao Zhang,[§] Wolter F. Jager,[‡] Ernst J.R. Sudhölter,[‡] Laurens D.A. Siebbeles,[†] Tom J. Savenije,[†] Shi Jin,[§] Ferdinand C. Grozema*[†]

[†]*Opto-Electronic Materials and Nano-Organic Chemistry, DelftChemTech, Delft University of Technology, Julianalaan 136, 2628 BL. Delft, The Netherlands*

[‡]*Nano-Organic Chemistry, DelftChemTech, Delft University of Technology, Julianalaan 136, 2628 BL. Delft, The Netherlands*

[§]*Department of Chemistry, City University of New York at Staten Island, 2800 Victoria Boulevard, Staten Island, NY 10314, USA*

E-mail: F.C.Grozema@tudelft.nl

Table of Contents

1 . General Experimental Section

1.1 Materials

All chemicals and solvents were purchased from commercial resources and used as received. ALIQUAT 336 was kindly provided by Cognis Corporation.

1.2 Molecular Identification

^{1}H NMR spectra were recorded on a Varian 600 MHz NMR spectrometer, with deuterated chloroform ($CDCl_3$) as solvent at 25 ^oC. The NMR graphs and data were collected by using MestreNova software. The peak at 7.26 ppm belonging to $CHCl_3$ residue was used as the internal standard. High resolution mass spectra (HRMS) were obtained at CUNY Mass Spectrometry Facility at Hunter College.

1.3 Fourier Transform Infrared Spectroscopy

Fourier transfer infrared spectra (FTIR) were recorded on a Bruker Vertex 70V spectrometer at the resolution of 1 $cm^{-1.}$

1.4 Fabrication of Thin Films

Solutions of neat perylenetetracarboxyldiimide (PDI) **7**, octa-dodecyloxy-substituted Cu (II) phthalocyanine) (CuPc) **9** and 50:50 (by weight) CuPc:PDI blend (with total active material concentrations of 4 mg/mL in chloroform were stirred at room temperature for 1 h under a nitrogen atmosphere inside a glovebox. The solutions were spin-coated onto clean rectangular (12 × 25 mm), 1 mm thick quartz substrates at 2500 rpm. Following spin-coating, the substrates were left in a covered glass Petri dish for one hour to allow for slow evaporation of the solvent, resulting in 80-90 nm thick films as measured by profilometry.

1.5 UV-Vis Absorption Spectroscopy

The transmission and reflection spectra of the films were recorded on a Perkin-Elmer Lambda 900 UV/Vis/NIR spectrophotometer equipped with an integrating sphere. The optical densities (absorption spectra) of the films were corrected for reflections using:

$$OD = -\log_{10}\left(\frac{I_T}{I_o - I_R}\right) \quad (1)$$

The attenuation spectrum (F_A) corresponds to the fraction of incident photons that is absorbed by the sample was calculated according to equation 2.

$$F_A = 1 - \left(\frac{I_T + I_R}{I_o}\right) \quad (2)$$

1.6 Pulse-Radiolysis Time-Resolved Microwave Conductivity

PR-TRMC technique has been extensively described elsewhere.[1] Briefly, the sample is irradiated with a short pulse of high-energy (3 MeV) electrons, which leads initially to a low (micromolar) concentration of positive and negative charge carriers uniformly distributed in the irradiated medium. After the incident pulse (1 – 50 ns duration), the conductivity of the sample is probed as a function of time by monitoring the attenuation of a reflected microwave power (frequency range between 28 and 38 GHz, maximum electric field strength in the sample 10 V/m). The fractional change in microwave power reflected by the cell is directly proportional to the change in conductivity, $\Delta\sigma$. The concentration of charges that is generated initially can be estimated using dosimetry measurements[2] combined with a charge-scavenging model. The charge carrier mobility can be calculated using this estimate of the charge carrier concentration. In presenting the data, a reasonable assumption has been made which is based on the insulation mantle of the saturated hydrocarbon surrounding cores, in which charge transport is highly one-dimensional along the columnar stacks. The one-dimensional, intercolumnar mobility for such a material is usually presented as $\Sigma\mu_{1D} = 3\Sigma\mu_{TRMC}$.

1.7 Time-Resolved Microwave Photoconductivity

FP-TRMC measurements were carried out using a custom-made liquid-nitrogen-cooled microwave cavity with a resonance frequency at ~8.4 GHz is employed. Samples were photoexcited with a 3 ns from an optical parametric oscillator pumped at 355 nm with a third harmonic of a Q-switched Nd:YAG laser (Vibrant II, Opotek). Photogeneration of mobile charge carriers in the sample results in an increase in the conductance, $\Delta G(t)$, and subsequently to absorption of microwave power by the sample. The time-dependent change of the photoconductance is obtained from the normalized change in reflected microwave power ($\Delta P(t)$/P) from the cavity, according to[3]

$$\frac{\Delta P(t)}{P} = -K\Delta G(t) \tag{3}$$

The sensitivity factor, K, is derived from the dimensions of the microwave cavity, and the geometrical and dielectric properties of the sample in the cavity. From the maximum change in the conductance (ΔG_{max}) and the incident light (I_o), the quantum yield for charge generation, φ, and the sum of the electron and hole mobilities, $\Sigma\mu$, can be calculated using

$$\varphi\Sigma\mu = \frac{\Delta G_{\max}}{I_o \beta e} \tag{4}$$

φ is related to the yield of charge carrier pairs formed per incident photon (IPCSE), η, simply by $\eta = \varphi F_A$.

2 . Synthesis and Molecular Identification

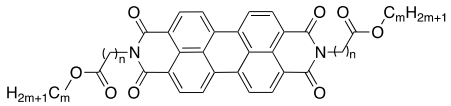

	n	m
1	1	12
2	2	11
3	3	10
4	4	9
5	5	8
6	6	7
7	11	2
8	5	2

PDI **1**[4] and **3**[5] were synthesized and characterized according to corresponding literature procedures. PDI **2**, **4**, **5** and **6** were prepared according to the following approach A:

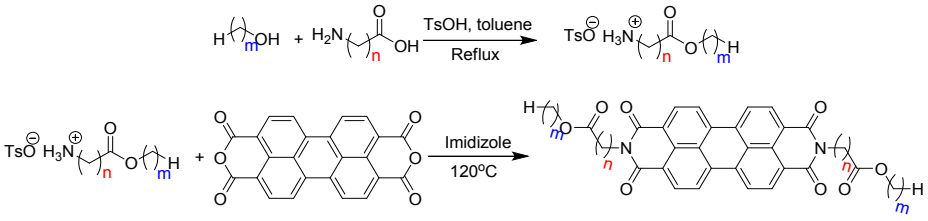

TsOH: *p*-toluenesulfonic acid

PDI **7** and **8** were synthesized according approach B:

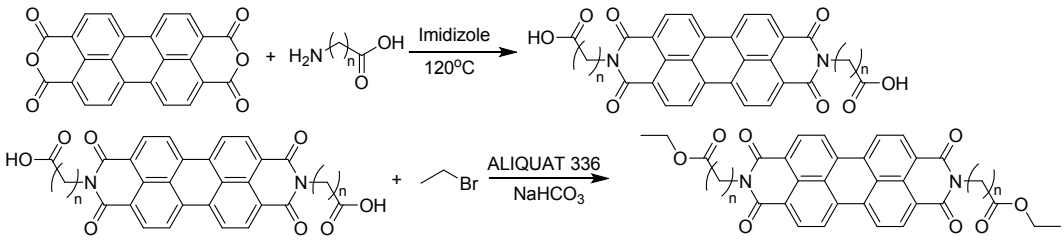

General procedure of approach A

First step

The corresponding alcohol (35 mmol), amino acid (20 mmol), *p*-toluenesulfonic acid monohydrate (22 mmol) in 50 mL toluene were placed in a Schlenk flask, which was evacuated and purged with N_2 three times. The reaction mixture was stirred at 110 °C for 8 hours. After cooling down to room temperature, the solvent was removed under reduced pressure, the residue was redissolved in acetone at 50 °C and the solution was left at 4 °C for crystallization. The resulting solid was collected by filtration and washed with cold acetone (2 x 5mL). Two repetitive recrystallization processes gave a white solid was obtained, which was dried at 70 °C overnight.

3-(undecyloxy)-3-oxopropylammonium toluenesulfonate: The corresponding alcohol and amino acid were 1-undecanol and *β*-alanine, m = 11, n = 2, yield 7.14 g (86%).

5-(nonyloxy)-5-oxopentylammonium toluenesulfonate: The corresponding alcohol and amino acid were 1-nonanol and 5-aminopentanoic acid, m = 9, n = 4, yield 7.30 g (88%).

6-(octyloxy)-6-oxohexylammonium toluenesulfonate: The corresponding alcohol and amino acid were 1-octanol and 6-aminohexanoic acid, m = 8, n = 5, yield 6.56 g (79%).

7-(heptyloxy)-7-oxoheptylammonium toluenesulfonate: The corresponding alcohol and amino acid were 1-heptanol and 7-aminoheptanoic acid, m = 7, n = 6, yield 7.47 g (90%).

Second step

The corresponding ester ammonium salt (2.4 mmol), 3,4:9,10-perylenetetracarobxyldianhydride (PDA) (1 mmol) and 6 g imidazole were placed in a Schlenk flask, which was evacuated and purged with N_2. The mixture was heated at 120 ^oC for 1 h with stirring. After cooling down to 90 ^oC, deionized water (15 mL) was added. The resulting solid was collected by vacuum filtration and dried at 60 ^oC overnight in a drying oven. The crude product was purified by column chromatography on silica gel (eluent: $CHCl_3$/acetone (95:5). PDI **2** could not be purified by column chromatography due to the low solubility. Instead, the crude product was washed with 3% K_2CO_3 aqueous solution until the solution became colorless under a UV light (no yellow-green emission).

General procedure of approach B

First step

A mixture of the corresponding amino acid (21 mmol), PDA (10 mmol) and imidazole (28 g) were placed in a Schlenk flask and heated at 120 ºC for 1 h under Ar atmosphere. The reaction mixture was diluted with deionized water while still warm (at 90 °C) and the resulting dark red solution was filtered to remove the trace amount of unreacted PDA. The filtrate was acidified with 2 M HCl aqueous solution to a pH value of 3-4. The resulting red precipitate was collected by vacuum filtration, washed with deionized water until the filtrate was neutral and dried at 75 ºC overnight in vacuum oven.

N, N'-di(1-carboxylpentyl)-3,4:9,10-perylenetetracarboxyldiimide: The corresponding amino acid was 6-aminohexanoic acid, n = 5, yield 5.93 g (96 %).
N, *N'*-di(1-carboxylundecyl)-3,4:9,10-perylenetetracarboxyldiimide: The corresponding amino acid was 12-aminododecanoic acid, n = 11, yield 7.54 g (96 %).

Second step

A solution of PDI dicarboxylic acid in 5% Na_2CO_3 (5 mL) was treated with ALIQUAT 336 in 2:1 (v/v) ethanol/H_2O mixture (10 mL) and stirred at room temperature for 30 min. The reaction mixture was extracted with $CHCl_3$ (3 × 10 mL) and the solvent was removed under reduced pressure. The

resulting solid was dried at 75 °C for 2 hours in a vacuum oven. The residue was redissolved in DMF (10 mL). 1-bromoethane (3 mmol) was added and the mixture was stirred for 12 h at room temperature. Methanol (40 mL) was added and the resulting precipitate was collected by vacuum filtration (for crystalline powder) or centrifugation (for sticky substance) and washed thoroughly with methanol. After being dried at 75 °C in a vacuum oven overnight, the crude product was purified by column chromatography on silica gel using $CHCl_3$/acetone (95:5) as the eluent.

***N,N'*-di(3-(undecyloxy)-3-oxopropyl)-3,4:9,10-perylenetetracarboxyldiimide (PDI 2)**: Yield 0.398 g (47%). ^{1}H NMR ($CDCl_3$, 600 MHz): δ (ppm) = 8.64 (d, J = 7.80 Hz, 4H, Ar), 8.54 (d, J = 7.80 Hz, 4H, Ar), 4.53 (t, J = 7.80 Hz, 4H, CH_2COOCH_2), 4.10 (t, J = 6.60 Hz, 4H, NCH_2CH_2COO), 2.82 (t, J = 7.20 Hz, 4H, NCH_2CH_2COO), 1.58 (m, 8H, $COOCH_2CH_2CH_2$), 1.31 – 1.19 (m, 28H, $COOCH_2CH_2CH_2(CH_2)_7CH_3$), 0.86 (t, J = 7.20 Hz, 6H, CH_3). HRMS $(M+H)^+$: calcd for $C_{52}H_{63}N_2O_8^+$ 843.4579; found 843.4581.

***N,N'*-di(5-(nonyloxy)-5-oxopentyl)-3,4:9,10-perylenetetracarboxyldiimide (PDI 4)**: Yield 0.304 g (36%). ^{1}H NMR ($CDCl_3$, 600 MHz): δ (ppm) = 8.25 (m, 4H, Ar), 7.98 (m, 4H, Ar), 4.16 (m, 4H, CH_2COOCH_2), 4.06 (t, J = 7.20 Hz, 4H, NCH_2CH_2), 2.43 (t, J = 7.20 Hz, 4H, $NCH_2CH_2CH_2CH_2COO$), 1.80 (m, 4H, $NCH_2CH_2CH_2$), 1.61 (m, 4H, $NCH_2CH_2CH_2$), 1.35 – 1.24 (m, 28H, $COOCH_2(CH_2)_7CH_3$), 0.85 (t, J = 7.20 Hz, 6H, CH_3). HRMS $(M+H)^+$: calcd for $C_{52}H_{63}N_2O_8^+$ 843.4579; found 843.4582.

***N,N'*-di(6-(octyloxy)-6-oxohexyl)-3,4:9,10-perylenetetracarboxyldiimide (PDI 5):** Yield 0.451 g (54%). ^{1}H NMR ($CDCl_3$, 600 MHz): δ (ppm) = 8.47 (d, J = 7.80 Hz, 4H, Ar), 8.30 (d, J = 7.80 Hz, 4H, Ar), 4.18 (t, J = 7.20 Hz, 4H, CH_2COOCH_2), 4.05 (t, J = 6.60 Hz, 4H, NCH_2CH_2), 2.35 (t, J = 7.20 Hz, 4H, $NCH_2CH_2CH_2CH_2CH_2COO$), 1.82 – 1.72 (m, 8H, $NCH_2CH_2CH_2CH_2CH_2COO$), 1.61 (m, 4H, $NCH_2CH_2CH_2$), 1.50 (m, 4H, $COOCH_2CH_2$), 1.33 – 1.25 (m, 20H, $COOCH_2CH_2(CH_2)_5CH_3$), 0.86 (t, J = 7.20 Hz, 6H, CH_3). HRMS $(M+H)^+$: calcd for $C_{52}H_{63}N_2O_8^+$ 843.4579; found 843.4581.

N,N'-di(7-(pentyloxy)-7-oxopentyl)-3,4:9,10-perylenetetracarboxyldiimide (PDI 6): Yield 0.390 g (46%). ^{1}H NMR ($CDCl_3$, 600 MHz): δ (ppm) = 8.37 (d, J = 7.80 Hz, 4H, Ar), 8.16 (d, J = 7.80 Hz, 4H, Ar), 4.15 (t, J = 7.80 Hz, 4H, CH_2COOCH_2), 4.05 (t, J = 7.20 Hz, 4H, NCH_2CH_2), 2.32 (t, J = 7.80 Hz, 4H, CH_2COO), 1.76 (m, 4H, CH_2CH_2COO), 1.67 (m, 4H, $CH_2CH_2CH_2COO$), 1.61 (m, 4H, NCH_2CH_2), 1.50 – 1.27 (m, 24H, $COOCH_2(CH_2)_5CH_3$ and $CH_2CH_2CH_2CH_2COO$), 0.86 (t, J = 7.20 Hz, 6H, CH_3). HRMS $(M+H)^+$: calcd for $C_{52}H_{63}N_2O_8^+$ 843.4579; found 843.4577.

***N,N'*-di(12-(ethyloxy)-12-oxododecyl)-3,4:9,10-perylenetetracarboxyldiimide (PDI 7)**: Yield 0.539 g (64%). ^{1}H NMR ($CDCl_3$, 600 MHz): δ (ppm) = 8.45 (d, J = 7.80 Hz, 4H, Ar), 8.28 (d, J = 7.80 Hz, 4H, Ar), 4.17 – 4.13 (m, 8H, CH_2COOCH_2 and NCH_2), 2.28 (t, J = 7.20 Hz, 4H, CH_2COO), 1.75

(m, 4H, CH_2CH$_2$COO), 1.61 (m, 4H, NCH$_2$CH_2), 1.46 – 1.23 (m, 34H, NCH$_2$CH$_2$(CH_2)$_7$CH$_2$CH$_2$COO and CH_3). HRMS (M+H)$^+$: calcd for $C_{52}H_{63}N_2O_8^+$ 843.4579; found 843.4583.

***N,N'*-di(6-(ethyloxy)-6-oxohexyl)-3,4:9,10-perylenetetracarboxyldiimide (PDI 8)**: Yield 0.411 g (61%). ^{1}H NMR ($CDCl_3$, 600 MHz): δ (ppm) = 8.23 (d, J = 7.80 Hz, 4H, Ar), 7.97 (d, J = 8.40 Hz, 4H, Ar), 4.15 – 4.10 (m, 8H, CH$_2$COOCH_2 and NCH_2CH$_2$), 2.36 (t, J = 7.80 Hz, 4H, CH_2COO), 1.80 – 1.71 (m, 8H, NCH$_2$CH$_2$CH_2CH_2CH$_2$COO), 1.50 (m, 4H, NCH$_2$CH_2CH$_2$), 1.26 (t, J = 7.20 Hz, 6H, CH_3). HRMS (M+H)$^+$: calcd for $C_{40}H_{39}N_2O_8^+$ 675.2701; found 675.2704.

3 . ^{1}H NMR Spectra

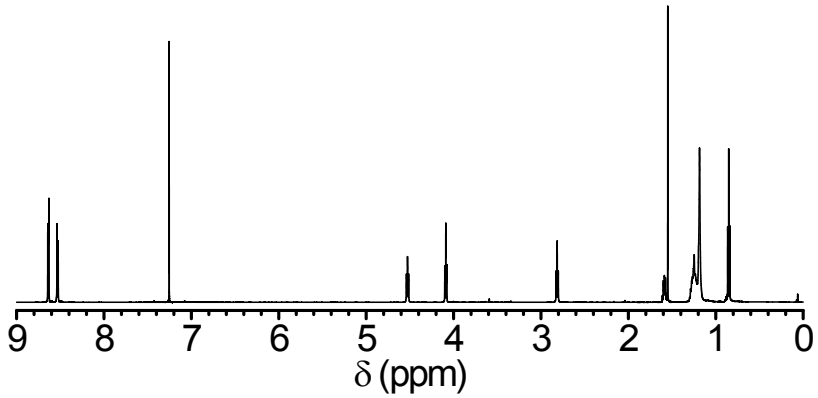

Figure S1. ^{1}H NMR spectrum of **2** (600 MHz, $CDCl_3$, 298 K).

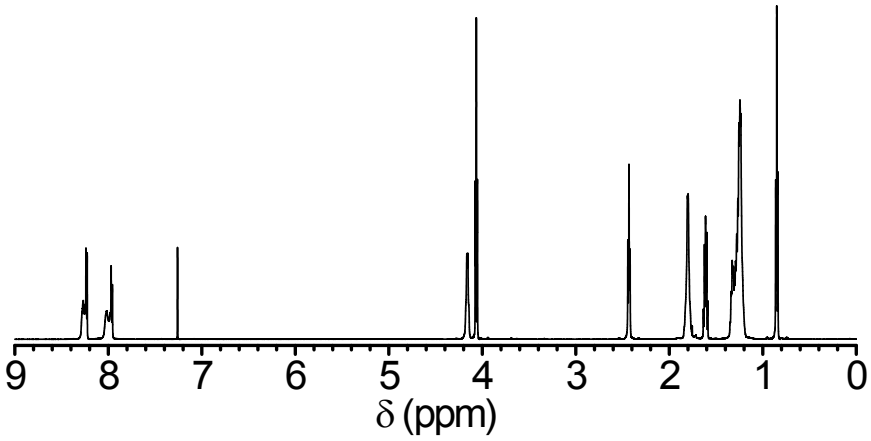

Figure S2. ^{1}H NMR spectrum of **4** (600 MHz, $CDCl_3$, 298 K).

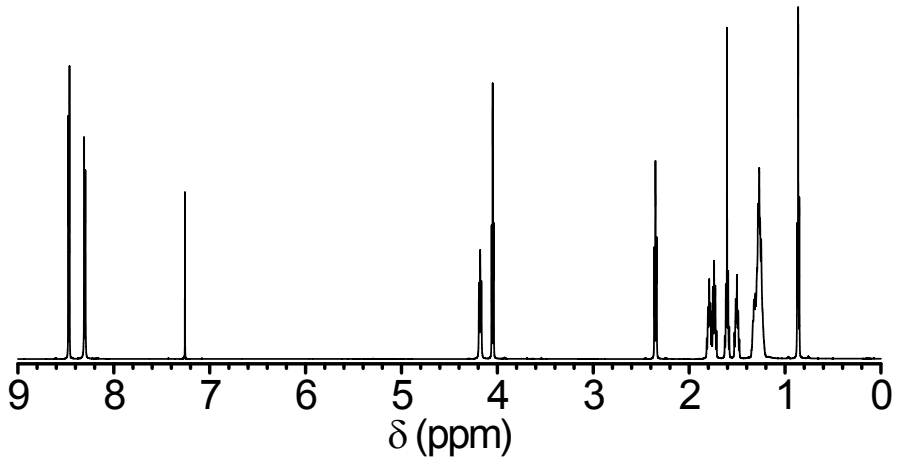

Figure S3. ^{1}H NMR spectrum of **5** (600 MHz, $CDCl_3$, 298 K).

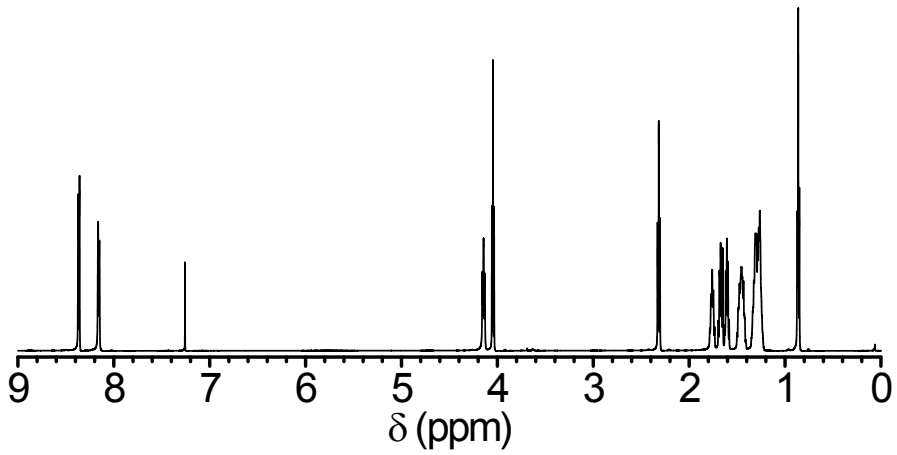

Figure S4. ^{1}H NMR spectrum of **6** (600 MHz, $CDCl_3$, 298 K).

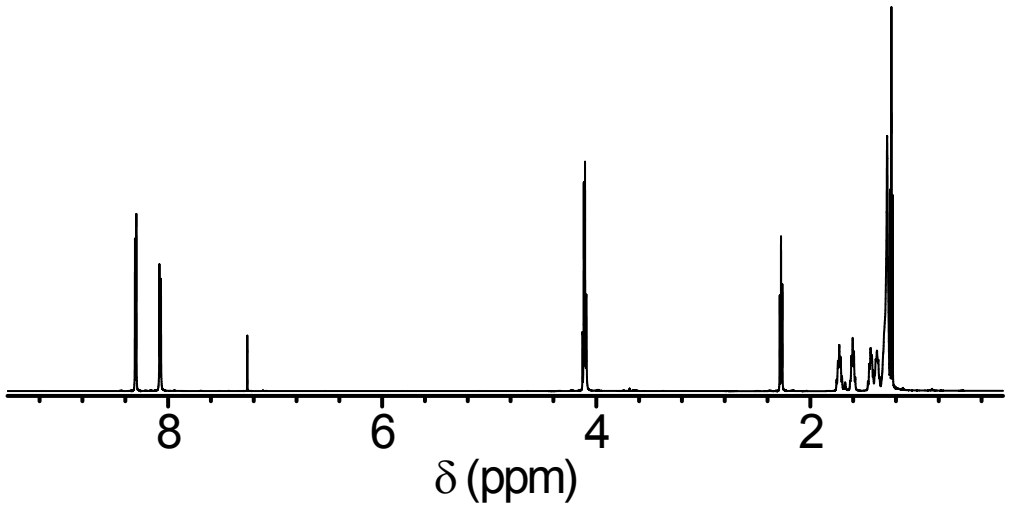

Figure S5. ^{1}H NMR spectrum of **7** (600 MHz, $CDCl_3$, 298 K).

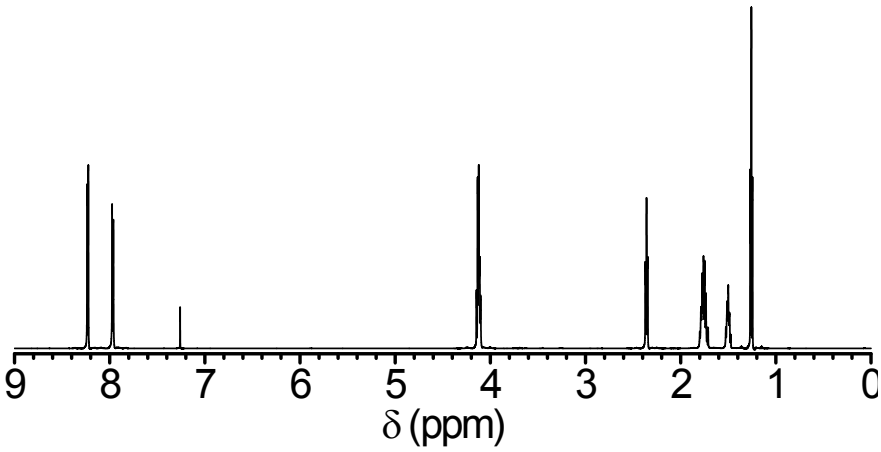

Figure S6. ^{1}H NMR spectrum of **8** (600 MHz, $CDCl_3$, 298 K).

4 . Infrared Spectra

Infrared spectra in solid state

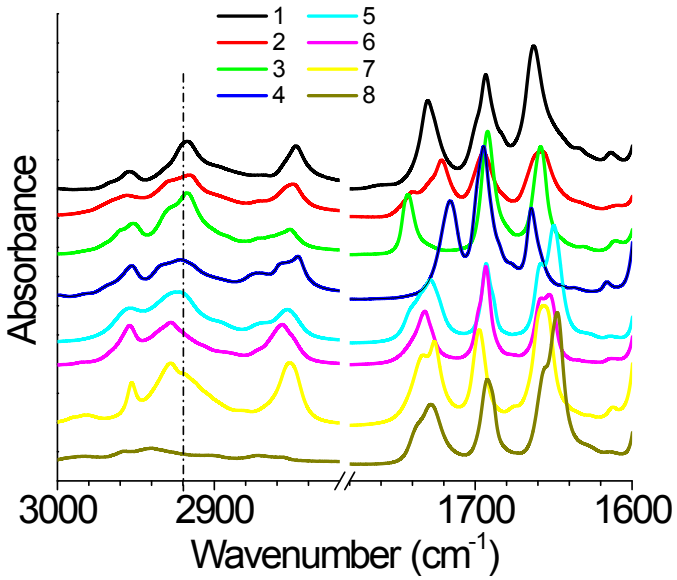

Figure S7. FTIR spectra of PDIs in solid state.

To probe ester dipole-dipole attractive interaction and conformation of polymethylene chains, FTIR spectra were collected on both solid and solution samples. The C-H and C=O stretching regions are shown in Figure S7. The dash line shows the frequency = 2920 cm^{-1}.

In order to qualitatively evaluate the strength of ester dipole-dipole interaction using FTIR, $\nu_{C=O}$ values of "free" ester groups are needed. Therefore, FTIR spectra of these compounds in dilute

chloroform solutions were also collected. (A model compound **1M** was used to in place of **1** due to its low solubility.)

1M: 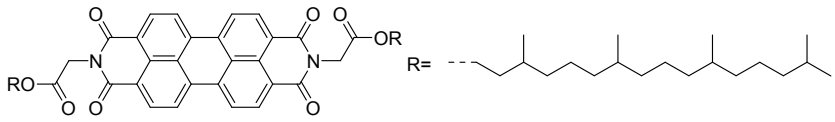

1M was synthesized according to approach **A** shown in the synthesis part. The corresponding alcohol was synthesized using a literature procedure.[6] A correction term was applied to the $\nu_{C=O}$ values obtained from chloroform solution as it is known that chloroform molecules are able to form hydrogen bonds with hydrogen bonding acceptors such as C=O groups, resulting in a lower $\nu_{C=O}$. The correct term was obtained by comparing the $\nu_{C=O}$ of ethyl acetate in hexane and that in chloroform. The $\nu_{C=O}$ of ethyl acetate in hexane solution was 1751 cm^{-1} while the corresponding value in chloroform was 1732 cm^{-1}. Therefore, a correct term of 19 cm^{-1} was yielded and added to $\nu_{C=O}$ values of PDI chloroform solutions. Such a corrected $\nu_{C=O}$ value qualitatively represents the $\nu_{C=O}$ of an unassociated ("free") ester group in a hydrocarbon environment.

Table 1. C=O stretching frequency ($\nu_{C=O}$) of PDIs **1-8**.

Compound	Solid $\nu_{C=O}$ (cm^{-1})[a]	$CHCl_3$ solution $\nu_{C=O}$ (cm^{-1})	"free" $\nu_{C=O}$ (cm^{-1})
1	1730	1746	1765
2	1740, 1721	1730	1749
3	1743	1727	1746
4	1716	1726	1745
5	1729, 1734, 1742	1725	1744
6	1732	1725	1744
7	1726, 1734	1725	1744
8	1728, 1738	1726	1745

[a] Positions of multiple $\nu_{C=O}$ were determined from second order derivative curves.

5. Melting Points of *n*-Alkyl Alkanate Ester Isomers

Structure of esters: 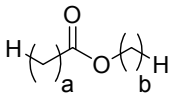

All melting points were obtained from Syracuse Research Corporation of Syracuse, New York (US) via SciFinder.

The melting point of decane (the *n*-alkane with similar molecular length) is -30 °C.

The melting point of undecane (the *n*-alkane with similar molecular mass) is -25.6 °C.

It is evident that all these ester isomers feature lower melting points than that of comparable *n*-alkanes. Furthermore, the melting point of an ester isomer is clearly a function of the position of the ester group in the molecule. When the ester group is located at the center of the chain, the molecule displays the lowest melting point. Each step the ester group moves away from the center of the chain, the melting point becomes higher. This may be explained by the desire of the ester groups to engage in attractive dipole-dipole interaction, which hinders the crystalline packing of all-anti polymethylene chains. It is expected such an effect is strongest when the ester group is at the center of the chain because in this case the largest number of methylene units will be under the direct and indirect influence.

Table 2. Melting points of *n*-alkyl alkanate ester isomers.

a	b	Melting point (°C)
1	7	-50.2
2	6	-57.5
3	5	-73.2
4	4	-92.8
5	3	-68.7
6	2	-66.1
7	1	-40

6 . AFM images

The AFM image shown in S8 exhibits the surface morphology of a ~80 nm thick CuPc **9** : PDI **7** blend layer spin-coated from $ChCl_3$ Although individual compounds dissolve readily the large variation in surface height indicates that the individual compound have a tendency to phase segregate.

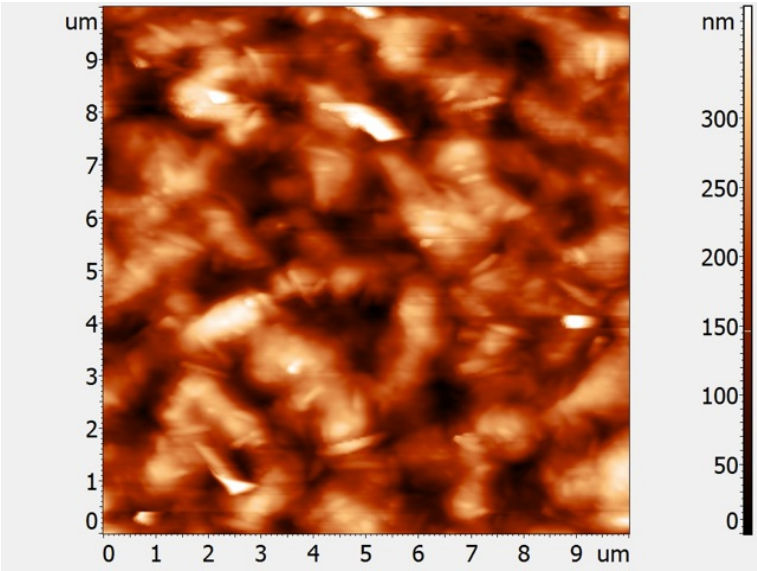

Figure S8. AFM image of blend of CuPc 9 : PDI 7 spin-coated on quartz substrate.

7 . Laser Fluence Dependence of $\varphi\Sigma\mu$ values

In order to understand in more detail the differences in the charge generation between two components, $\varphi\Sigma\mu$ values for excitation at 500 nm and 700 nm for blend CuPc **9** :PDI **7** was compared (Figure S9). The product $\varphi\Sigma\mu$ shows a decrease in its magnitude with an increase in laser fluence, which is attributed to higher order decay processes, such as exciton-exciton annihilation and/or bimolecular charge carrier recombination.[7] However, for a fluence below 7×10^{13} photons/cm^2/pulse the $\varphi\Sigma\mu$ values are constant indicating that photoconductance is predominantly due to first order geminate charge recombination and/or trapping. Note that the maximum in photoductance on excitation at 500 nm is somewhat higher than excitation at 700 nm. This implies that quantum yield for charge generation, φ, upon excitation at 500 nm is slightly higher as compared to excitation at 700 nm in CuPc **9** : PDI **7** blend.

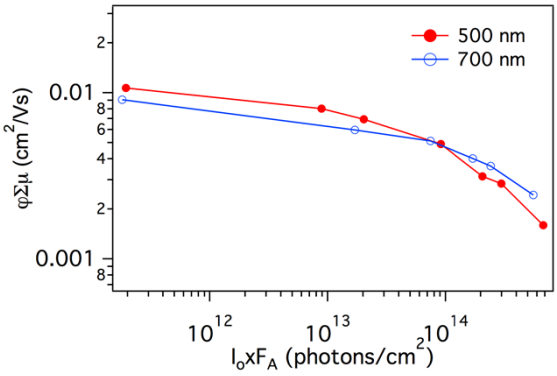

Figure S9. The product of the quantum yield per absorbed photon (φ) and the sum of the charge carrier mobilities ($\Sigma\mu$) versus incident intensity normalized to the optical absorption at 500 nm and 700 nm for blend of CuPc 9 : PDI 7.

8 . References

(1) Warman, J. M.; van de Craats, A. M. Charge Mobility in Discotic Materials Studied by PR-TRMC. *Mol. Cryst. Liq. Cryst.* **2003**, *396*, 41-72.

(2) Warman, J. M.; de Haas, M. P.; Dicker, G.; Grozema, F. C.; Piris, J.; Debije, M. G. Charge Mobilities in Organic Semiconducting Materials Determined by Pulse-Radiolysis Time-Resolved Microwave Conductivity: π-Bond-Conjugated Polymers versus π-π-Stacked Discotics. *Chem. Mater.* **2004**, *16*, 4600-4609.

(3) Kroeze, J. E.; Savenije, T. J.; Vermeulen, M. J. W.; Warman, J. M. Contactless Determination of the Photoconductivity Action Spectrum, Exciton Diffusion Length, and Charge Seperation Efficiency in Polythiphene-Sensitized TiO_2 Bilayers. ***J. Phys. Chem. B*** **2003**, ***107***, 7696-7705.

(4) Xu, Y. J.; Leng, S. W.; Xue, C. M.; Sun, R. K.; Pan, J.; Ford, J.; Jin, S. A Room Temperature Liquid-Crystalline Phase with Crystalline π Stacks. ***Angew. Chem. Int. Ed.*** **2007**, ***46***, 3896-3899.

(5) Xue, C.; Jin, S. Exceptionally Strong Electronic Coupling in Crystalline Perylene Diimides via Tuning.*Chem. Mater.* **2011**, *23*, 2689-2692.

(6) Fong, C.; Wells, D.; Krodkiewska, I.; Hartley, P. G.; Drummond, C. J. New Role for Urea as Surfactant Headgroup Promoting Self-Assembly in Water. *Chem. Mater.* **2006**, *18*, 594-597.

(7) **Kroeze,** J.E.; **Koehorst,** R.B.M, **Savenije**, T.J. **Singlet and Triplet Exciton Diffusion in a Self-Organizing Porphyrin Antenna Layer.** ***Adv. Funct. Mater.*** **2004, 14,** 992-998.